Comparison between the performance of quantitative flow ratio and perfusion imaging for diagnosing myocardial ischemia

Diemen, P.A. van; Driessen, R.S.; Kooistra, R.A.; Stuijfzand, W.J.; Raijmakers, P.G.; Boellaard, R.; ... ; Knaapen, P.

JACC: CARDIOVASCULAR IMAGING VOL. 13, NO. 9, 2020

PUBLISHED BY ELSEVIER

ORIGINAL RESEARCH

Comparison Between the Performance of Quantitative Flow Ratio and Perfusion Imaging for Diagnosing Myocardial Ischemia

Pepijn A. van Diemen, MD,[a] Roel S. Driessen, MD,[a] Rolf A. Kooistra, PhD,[b] Wynand J. Stuijfzand, MD,[a] Pieter G. Raijmakers, MD, PhD,[c] Ronald Boellaard, MD, PhD,[c] Stefan P. Schumacher, MD,[a] Michiel J. Bom, MD,[a] Henk Everaars, MD,[a] Ruben W. de Winter, MD,[a] Peter M. van de Ven, PhD,[d] Johan H. Reiber, MD, PhD,[b] James K. Min, MD,[e] Jonathan A. Leipsic, MD,[f] Juhani Knuuti, MD, PhD,[g] Richard S. Underwood, MD, PhD,[h] Albert C. van Rossum, MD, PhD,[a] Ibrahim Danad, MD, PhD,[a] Paul Knaapen, MD, PhD[a]

ABSTRACT

OBJECTIVES This study compared the performance of the quantitative flow ratio (QFR) with single-photon emission computed tomography (SPECT) and positron emission tomography (PET) myocardial perfusion imaging (MPI) for the diagnosis of fractional flow reserve (FFR)–defined coronary artery disease (CAD).

BACKGROUND QFR estimates FFR solely based on cine contrast images acquired during invasive coronary angiography (ICA). Head-to-head studies comparing QFR with noninvasive MPI are lacking.

METHODS A total of 208 (624 vessels) patients underwent technetium-^{99}m tetrofosmin SPECT and [^{15}O]H_2O PET imaging before ICA in conjunction with FFR measurements. ICA was obtained without using a dedicated QFR acquisition protocol, and QFR computation was attempted in all vessels interrogated by FFR (552 vessels).

RESULTS QFR computation succeeded in 286 (52%) vessels. QFR correlated well with invasive FFR overall ($R = 0.79$; $p < 0.001$) and in the subset of vessels with an intermediate (30% to 90%) diameter stenosis ($R = 0.76$; $p < 0.001$). Overall, per-vessel analysis demonstrated QFR to exhibit a superior sensitivity (70%) in comparison with SPECT (29%; $p < 0.001$), whereas it was similar to PET (75%; $p = 1.000$). Specificity of QFR (93%) was higher than PET (79%; $p < 0.001$) and not different from SPECT (96%; $p = 1.000$). As such, the accuracy of QFR (88%) was superior to both SPECT (82%; $p = 0.010$) and PET (78%; $p = 0.004$). Lastly, the area under the receiver operating characteristics curve of QFR, in the overall sample (0.94) and among vessels with an intermediate lesion (0.90) was higher than SPECT (0.63 and 0.61; $p < 0.001$ for both) and PET (0.82; $p < 0.001$ and 0.77; $p = 0.002$), respectively.

CONCLUSIONS In this head-to-head comparative study, QFR exhibited a higher diagnostic value for detecting FFR-defined significant CAD compared with perfusion imaging by SPECT or PET. (J Am Coll Cardiol Img 2020;13:1976–85)

From the [a]Department of Cardiology Amsterdam UMC, Vrije Universiteit Amsterdam, Amsterdam, the Netherlands; [b]Medis Medical Imaging Systems, Leiden, the Netherlands; [c]Department of Radiology, Nuclear Medicine, and PET Research, Amsterdam UMC, Vrije Universiteit Amsterdam, Amsterdam, the Netherlands; [d]Department of Epidemiology and Biostatistics, Amsterdam UMC, Vrije Universiteit Amsterdam, Amsterdam, the Netherlands; [e]Institute for Cardiovascular Imaging, Weill-Cornell Medical College, New York-Presbyterian Hospital, New York, New York; [f]Department of Medicine and Radiology, University of British Columbia, Vancouver, British Columbia, Canada; [g]Turku PET Centre, Turku University Hospital and University of Turku, Turku, Finland; and the [h]Department of Nuclear Medicine, Royal Brompton Hospital, London, United Kingdom. The authors have reported that they have no relationships relevant to the contents of this paper to disclose. James Udelson, MD, served as Guest Editor for this paper.

ISSN 1936-878X/$36.00 https://doi.org/10.1016/j.jcmg.2020.02.012

The landmark FAME (Fractional Flow Reserve versus Angiography for Multivessel Evaluation) trial demonstrated fractional flow reserve (FFR)–guided revascularization to be superior in terms of patient outcome compared with an angiography-based approach (1). As such, guidelines advocate the use of FFR measurements to detect hemodynamically significant coronary artery disease (CAD) (2). However, FFR usage is limited to intervention centers as it requires the use of an intracoronary pressure wire. Quantitative flow ratio (QFR) is a technique that estimates FFR based on a 3-dimensional (3D) coronary model reconstructed from cine contrast images obtained during invasive coronary angiography (ICA) and fast computational fluid dynamics that obviate the need for intracoronary pressure wires or hyperemic conditions (3). The FAVOR-II (Functional Diagnostic Accuracy of Quantitative Flow Ratio in Online Assessment of Coronary Stenosis) trials demonstrated that QFR accurately depicted lesion-specific, FFR-defined significant CAD (4,5). Besides invasive diagnostic tools, myocardial perfusion imaging (MPI) with either single-photon emission computed tomography (SPECT) or positron emission tomography (PET) allows for the functional assessment of CAD in a noninvasive manner (6). An invasive strategy by ICA with functional testing (e.g., QFR) and a noninvasive approach using MPI are both viable diagnostic options for patients with suspected CAD (2). Currently, a head-to-head comparison between the diagnostic value of QFR and MPI when referenced by FFR is lacking.

METHODS

STUDY POPULATION. This is a substudy of the prospective comparison of coronary CT angiography, SPECT, PET, and hybrid imaging for the diagnosis of ischemic heart disease determined by FFR (PACIFIC [Comparison of Cardiac Imaging Techniques for Diagnosing Coronary Artery Disease]; NCT01521468) (7). A total of 208 patients without a history of CAD (i.e., previous coronary revascularization or myocardial infarction) but suspected of having CAD underwent coronary CT angiography, SPECT, and PET before ICA with interrogation of all major coronary arteries by FFR, regardless of stenosis severity. For the present study, QFR computation was attempted in all coronary arteries in which FFR was obtained. The PACIFIC trial was approved by the institutional Medical Ethics Committee and complied with the Declarations of Helsinki. All participants provided written informed consent.

SPECT. SPECT scans were obtained using a dual-head hybrid SPECT/CT machine (Symbia T2, Siemens Medical Solutions, Erlanger, Germany). As previously described, imaging entailed a 2-day stress (intravenous adenosine 140 μg/kg/min) and rest protocol using a weight-adjusted dose of 370 to 550 MBq of ^{99}mTc tetrofosmin as a radiopharmaceutical (7). Uptake images were acquired using electrocardiographic gating and followed by a low-dose CT scan for attenuation correction. A blinded core laboratory (Royal Brompton Hospital, London, United Kingdom) assessed SPECT uptake images. A 17-segment model was used, in which each segment of the rest and stress scans was visually graded for the presence of a perfusion defect scored on a 5-point scale (0: normal; 1: mildly decreased; 2: moderately decreased; 3: severely decreased; 4: absence of uptake) (8). A summed difference score (SDS) was calculated by subtracting the summed rest score from the summed stress score. An SDS ≥2 within 1 vascular territory was considered indicative of myocardial ischemia.

PET. [^{15}O]H_2O PET perfusion images were acquired on a hybrid PET/CT device (Philips Gemini TF64, Philips Healthcare, Best, the Netherlands) as previously published (7). Absolute myocardial blood flow in ml/min/g was obtained using a dynamic rest and stress protocol using intravenous adenosine (140 μg/kg/min) as a hyperemic agent and 370 MBq of [^{15}O]H_2O as a radioactive tracer. Vascular territories were defined according to the standardized 17-segment model of the American Heart Association (8). A blinded core laboratory (Turku University Hospital, Turku, Finland) studied reconstructed PET scans for the presence of ischemia. A hyperemic myocardial blood flow of ≤2.3 ml/min/g in at least 2 adjacent segments within 1 vascular territory was used to define myocardial ischemia (7).

ICA AND FFR. At least 2 orthogonal projections per evaluated coronary artery were obtained. Epicardial vasodilation was achieved by an intracoronary

ABBREVIATIONS AND ACRONYMS

3D-QCA = 3-dimensional quantitative coronary angiography
CAD = coronary artery disease
CT = computed tomography
FFR = fractional flow reserve
ICA = invasive coronary angiography
ICC = intraclass coefficients
MPI = myocardial perfusion imaging
PET = positron emission tomography
QFR = quantitative flow ratio
SDS = summed difference score
SPECT = single-photon emission computed tomography

The authors attest they are in compliance with human studies committees and animal welfare regulations of the authors' institutions and Food and Drug Administration guidelines, including patient consent where appropriate. For more information, visit the *JACC: Cardiovascular Imaging* author instructions page.

Manuscript received September 20, 2019; revised manuscript received December 12, 2019, accepted February 5, 2020.

FIGURE 1 Study Flowchart

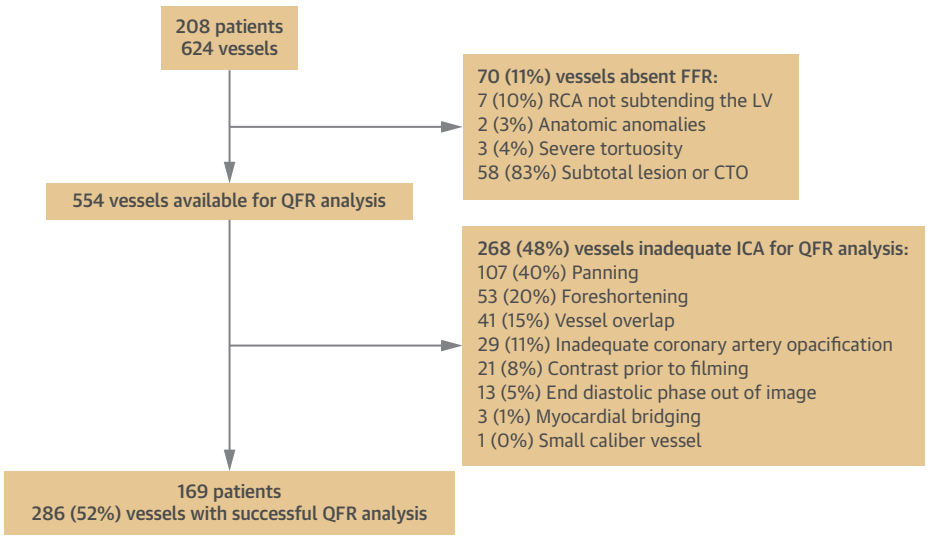

Study flowchart demonstrating the number of vessels included in the present study and reasons quantitative flow ratio (QFR) could not be computed. CTO = chronic coronary total occlusion; FFR = fractional flow reserve; ICA = invasive coronary angiography; LV = left ventricle; RCA = right coronary artery.

injection of 0.2 mg nitroglycerine before contrast injection. ICA images were obtained without adherence to a dedicated QFR acquisition protocol (i.e., no standardized views, varying magnification, collimation, and panning at the discretion of the operator). After visual assessment, coronary arteries were interrogated by FFR, regardless of stenosis severity, except for occluded or subtotal lesions in which wire passage was not deemed feasible by the operator. Hyperemia was induced via infusion of intracoronary (150 μg) or intravenous (140 μg/kg/min) adenosine. FFR was calculated as the ratio of mean distal intracoronary pressure and mean arterial pressure. A lesion with an FFR ≤0.80 was deemed significant.

THREE-DIMENSIONAL QUANTITATIVE CORONARY ANGIOGRAPHY AND QFR COMPUTATION. QFR computation was performed by a blinded core laboratory (ClinFact Medis Specials bv., Leiden, the Netherlands) using the QAngio XA 3D/QFR V1.2 solution software package (Medis Medical Imaging Systems bv., Leiden, the Netherlands). An end-diastolic frame of 2 projections at least 25° apart from the same coronary artery was used to reconstruct a 3D model of the vessel. This model allowed for 3D quantitative coronary angiography (3D-QCA), which resulted in anatomical lesion information such as diameter stenosis percentage and lesion length. The reference vessel was constructed by fitting the healthy segments proximally and distally to the lesion of interest. An estimation of the contrast velocity was obtained by frame count analysis that indicated the frames where contrast entered and exited the analyzed part of the vessel. The estimated contrast velocity was subsequently converted into a virtual hyperemic flow velocity that allowed for computation of the pressure drop along the vessel, which permitted QFR reading at any point along the vessel. For the present study, QFR computation was attempted in all vessels with documented FFR. Similar to FFR, a QFR of ≤0.80 was deemed significant. Furthermore, lesions with a diameter stenosis of 30% to 90%, as defined by 3D-QCA, were considered to be of intermediate severity.

STATISTICAL ANALYSIS. Continuous variables are presented as mean ± SD or median (interquartile range) where appropriate, whereas categorical variables are expressed as frequencies with percentages. Diagnostic performance measures were compared using generalized estimating equations with an exchangeable working correlation structure (sensitivity, specificity, and accuracy) or independent working correlation structure (positive predictive value and negative predictive value). In addition, sensitivity, specificity, and accuracy of QFR, SPECT, and PET were compared using the paired McNemar test. A Bonferroni correction, which multiplied the p value by 2, was applied to account for multiple testing. Areas under the receiver operating characteristic curves were compared with the DeLong

TABLE 1 Baseline Characteristics (N = 169)

Male	101 (60)
Age, yrs	58 ± 9
BMI, kg/m^2	27.0 ± 3.6
Cardiovascular risk factors	
Diabetes mellitus	29 (17)
Hypertension	83 (49)
Hypercholesterolemia	70 (41)
History of tobacco use	79 (47)
Family history of CAD	86 (51)
Medications	
Acetylic acid	149 (88)
Beta-blockers	110 (65)
Calcium-channel blockers	50 (30)
Long-acting nitrates	20 (12)
Statins	132 (78)
ACE inhibitors	34 (20)
AR blockers	35 (21)
Symptoms	
Typical AP	60 (36)
Atypical AP	49 (28)
Nonspecific chest pain	60 (36)

Values are n (%) or mean ± SD.

ACE = angiotensin-converting enzyme; AP = angina pectoris; AR = angiotensin receptor; BMI = body mass index; CAD = coronary artery disease.

method. Associations between QFR and FFR were quantified using Spearman's rank correlations. Agreement between QFR and FFR was assessed using intraclass coefficients (ICCs) and Bland-Altman analyses. A 2-way mixed effects model was used to determine the ICCs for single measures. Lastly, bias between QFR and FFR was assessed using paired Student's *t*-tests. All analyses were performed using IBM SPSS (SPSS Statistics 26, IBM, Armonk, New York) and MedCalc (MedCalc Software 11.6.0.0, Mariakerke, Belgium).

RESULTS

PATIENT AND LESION CHARACTERISTICS. A total of 624 vessels (208 patients) were evaluated for inclusion in the present study. FFR measurements were absent in 70 (11%) vessels and were therefore excluded, leaving a total of 552 vessels in which QFR computation was attempted (**Figure 1**). ICA was obtained without using a dedicated QFR acquisition protocol. Therefore, issues related to ICA images (e.g., panning, foreshortening, or vessel overlap) were the main drivers of failure to compute QFR. Finally, QFR analysis was successful in 286 (52%) vessels among 169 patients. PET imaging was not completed due to claustrophobia in 2 of these patients, whereas SPECT scanning could not be performed due to technical difficulties in 1 patient. Patient and angiographic characteristics are presented in **Tables 1 and 2**. Of the vessels included, 173 (60%) exhibited an intermediate lesion as defined by 3D-QCA. FFR and QFR had skewed distributions, with medians of 0.93 (interquartile range: 0.84 to 0.97) and 0.96 (interquartile range: 0.84 to 1.00), respectively. A lesion with an FFR below the cutoff that defined ischemia was present in 21% of the vessels.

OVERALL DIAGNOSTIC PERFORMANCE OF QFR AND MPI. The overall diagnostic performance of QFR, SPECT, and PET is presented in **Table 3**, whereas diagnostic performance of SPECT and PET among included and excluded vessels is displayed in Supplemental Table 1. QFR exhibited a significantly higher area under the curve (0.94) compared with SPECT (0.63; $p < 0.001$) and PET (0.82; $p < 0.001$) (**Figure 2**). Sensitivity of QFR (70%) was superior to SPECT (29%; $p < 0.001$) and did differ from PET (75%; $p = 1.000$). The specificity of QFR was 93%, which was similar to SPECT (96%; $p = 1.000$) but higher than PET (79%; $p < 0.001$). The negative predictive value of QFR (92%) was higher than SPECT (84%; $p < 0.001$) and not different from PET (92%; $p = 1.000$). In contrast, the positive predictive value of QFR (73%) was comparable to SPECT (68%; $p = 0.086$) but superior to PET (48%; $p < 0.001$). As such, the accuracy of QFR (88%) was superior to both SPECT (82%; $p = 0.010$) and PET (78%; $p = 0.004$), whereas the accuracy of SPECT and PET did not differ ($p = 0.905$). QFR, SPECT, and PET results stratified according to FFR subgroups are displayed in Supplemental Table 2.

DIAGNOSTIC PERFORMANCE OF QFR AND MPI AMONG VESSELS WITH A LESION OF INTERMEDIATE SEVERITY. Among vessels with an intermediate lesion, QFR had a higher area under the curve (0.90) compared with SPECT (0.63; $p < 0.001$) and PET (0.77; $p = 0.002$) (**Figure 2**). QFR (72%) exhibited a superior sensitivity compared with SPECT (30%; $p < 0.001$), although the sensitivity was not different from PET (77%; $p = 1.000$). Conversely, specificity of QFR (86%) was similar to SPECT (90%; $p = 1.000$) but superior to PET (70%; $p = 0.004$). A negative predictive value of 85% was observed for QFR, which was higher than that of SPECT (70%; $p < 0.001$) but comparable to PET (85%; $p = 1.000$). QFR (73%) exhibited a superior positive predictive value in comparison with PET (58%; $p = 0.034$), whereas it was similar to SPECT (62%; $p = 0.496$). Diagnostic accuracy of QFR (81%) was significantly higher than that of SPECT (69%; $p = 0.008$) but did not differ from PET (72%; $p = 0.112$). Lastly, SPECT and PET had a similar accuracy ($p = 0.597$).

TABLE 2 Lesion Characteristics

	Overall (N = 286)	Intermediate Lesions (n = 173)
Vessel		
RCA territory	87 (30)	39 (23)
RCA	77 (27)	34 (87)
RDP	8 (3)	1 (3)
RPL	2 (1)	4 (10)
LAD territory	125 (44)	95 (55)
LAD	122 (43)	93 (98)
D	3 (1)	2 (2)
Circumflex territory	74 (26)	39 (23)
Cx	58 (20)	26 (67)
OM	12 (4)	10 (26)
AL	4 (1)	3 (8)
Anatomical		
DS%	37 ± 16	47 ± 13
Intermediate lesions (DS% 30–90)	173 (60)	173 (100)
Lesion length, mm	18 ± 13	22 ± 14
MLD, mm	1.7 ± 0.6	1.4 ± 0.4
Functional		
QFR	0.96 (0.84-1.00)	0.88 (0.76-0.95)
QFR ≤0.80	59 (21)	59 (34)
FFR	0.93 (0.84-0.97)	0.86 (0.75-0.94)
FFR ≤0.80	61 (21)	60 (35)

Values are n (%), median (interquartile range), or mean ± SD.

AL = anterolateral; Cx = left circumflex artery; D = diagonal, DS = diameter stenosis; FFR = fractional flow reserve; LAD = left anterior descending; MLD = minimal lumen diameter; OM = obtuse marginal; QFR = quantitative flow ratio; RCA = right coronary artery; RDP = ramus descending posterior; RPL = right posterolateral.

CORRELATION AND AGREEMENT BETWEEN QFR AND FFR. Overall, a significant correlation between QFR and FFR was observed ($R = 0.79$; $p < 0.001$), with a mean difference of -0.02 ± 0.09 ($p < 0.001$) and good agreement (ICC: 0.80; $p < 0.001$) (Figure 3). When analyses were performed stratified according to vascular territory, similar agreement between QFR and FFR was observed (Figure 4). Considering only vessels with an intermediate lesion, a significant correlation ($R = 0.76$; $p < 0.001$) between QFR and FFR was again noted, with a mean difference of -0.01 ± 0.11 ($p = 0.103$) and good agreement (ICC: 0.76; $p < 0.001$) (Figure 3).

DISCUSSION

The present study was the first to compare the diagnostic performance of QFR with the MPI modalities of SPECT and PET in a head-to-head fashion against a reference of invasive FFR measurements. QFR and FFR showed good correlation and agreement. Overall, the diagnostic accuracy of QFR was higher than SPECT and PET; however, when solely considering vessels with an intermediate lesion, the accuracy of QFR was superior to SPECT, but similar to PET. Nevertheless, comparative area under the receiver-operating characteristic curves analyses demonstrated that QFR exhibited a superior performance for diagnosing FFR-defined significant CAD compared with SPECT and PET, overall and among vessels with an intermediate lesion (Central Illustration).

DIAGNOSTIC PERFORMANCE OF QFR AND MPI. A recent meta-analysis of 819 (969 vessels) prospectively enrolled patients demonstrated QFR to have a sensitivity of 84% and specificity of 88% when referenced by FFR (9). Sensitivity seemed to be higher among studies that computed QFR online (i.e., directly during ICA) compared with off-line computation after obtaining ICA. Online computation might lead to a more favorable QFR and FFR concordance because the wire location can be directly matched by the operator. Diagnostic values of the present study

TABLE 3 Diagnostic Performance of QFR and MPI, Overall and Among Vessels With a Lesion of Intermediate Severity

	QFR	SPECT	p Value*	PET	p Value*
Overall					
Sensitivity	70 (57-81)	29 (18-42)	<0.001/<0.001†	75 (62-85)	1.000 /1.000†
Specificity	93 (89-96)	96 (93-98)	1.000/1.000†	79 (73-84)	<0.001/<0.001†
NPV	92 (89-94)	84 (81-86)	<0.001	92 (88-95)	1.000
PPV	73 (62-82)	68 (49-82)	0.086	48 (41-56)	<0.001
Accuracy	88 (84-92)	82 (77-87)	0.010 /0.00†	78 (73-83)	0.004/0.006†
Intermediate lesions					
Sensitivity	72 (59-83)	30 (19-43)	<0.001/<0.001†	77 (64-87)	1.000/1.000†
Specificity	86 (78-92)	90 (83-95)	1.000/0.848†	70 (60-78)	0.004/0.020†
NPV	85 (79-90)	70 (67-74)	<0.001	85 (78-90)	1.000
PPV	73 (62-81)	62 (45-76)	0.496	58 (50-65)	0.034
Accuracy	81 (74-86)	69 (61-76)	0.008/0.015†	72 (65-79)	0.112/0.154†

Values are % (95% confidence interval). *The p value concerns the comparison with QFR. †The p value calculated using the paired McNemar-test; every p value has been multiplied by 2 to account for multiple testing.

MPI = myocardial perfusion imaging; NPV = negative predictive value; PET = positron emission tomography; PPV = positive predictive value; SPECT = single-photon emission computed tomography; other abbreviations as in Tables 1 and 2.

were in line with the values observed in the WIFI-II (Wire-Free Functional Imaging-II Study) (sensitivity 77%, specificity 86%), which similarly analyzed QFR in an off-line fashion (10). With regard to MPI, the observed per-vessel sensitivity of SPECT (29%) and PET (75%) appeared to be lower compared with the sensitivity reported in the PACIFIC main paper (39% and 81%, respectively), whereas specificity and accuracy were similar. Importantly, the present study excluded vessels with subtotal or chronic coronary total occlusion because QFR analysis would not be clinically relevant; however, these vessels would have been correctly assessed by MPI in most cases, augmenting sensitivity (Supplemental Table 1). Nevertheless, including these vessels would not have changed the comparison between QFR and MPI because these vessels would also be classified correctly by ICA in conjunction with QFR.

QFR VERSUS MPI. QFR appears to have a superior diagnostic value for detecting FFR-defined significant CAD compared with SPECT and quantitative [^{15}O]H_2O PET, which is worth analyzing. The concordance between QFR and FFR is not surprising because both techniques were developed to solely assess epicardial lesion specific significance. MPI takes the whole coronary vasculature into account, assessing both epicardial stenosis and diffuse and/or small-vessel disease, which do not cause focal pressure gradients and therefore go undetected by FFR or QFR (11,12). As such, discordant invasive and noninvasive results do not necessarily depict inaccuracies of either technique, but more likely reflect the ability of the modalities to assess different stages and aspects of the atherosclerotic process (12). For example, impaired FFR with normal perfusion can be observed in patients with focal stenosis but preserved microvasculature; in contrast, normal FFR with diminished perfusion can be seen in patients with small-vessel disease (11,12). Therefore, a simplified diagnostic comparison using binary results (i.e., normal vs. abnormal) does not do justice to the complex relationship between atherosclerosis and myocardial perfusion. Nevertheless, a FFR-guided revascularization strategy is the only approach that leads to a beneficial outcome in patients with stable CAD. Therefore, determining the value of diagnostic techniques to assess the FFR revascularization threshold is of clinical importance (13). The higher accuracy of QFR compared with SPECT is driven by a lower rate of false negative findings, whereas specificity is similar. A growing body of evidence shows SPECT has a poor sensitivity when referenced by FFR (7,14,15). Sensitivity of SPECT is hampered by the relatively low spatial resolution and unfavorable tracer kinetics, which cause subtle perfusion defects to remain undetected (6). Conversely, quantitative PET results in a higher rate of false positive findings compared with QFR, whereas sensitivity is comparable. These false positive findings are presumably caused by diffuse atherosclerosis and/or small vessel disease, which do not lead to pressure gradients but do result in lower myocardial perfusion (12).

CLINICAL APPLICABILITY. QFR enables sites that obtain ICA to functionally evaluate CAD, because it solely relies on cine contrast images. Contemporary guidelines present an invasive approach by ICA in conjunction with functional assessment (e.g., QFR), as well as a noninvasive approach using MPI (e.g., SPECT/PET) as feasible diagnostic pathways for patients with an abnormal coronary CT angiography or

FIGURE 2 Diagnostic Performance of QFR, SPECT, and PET, Overall and Among Vessels With an Intermediate Lesion

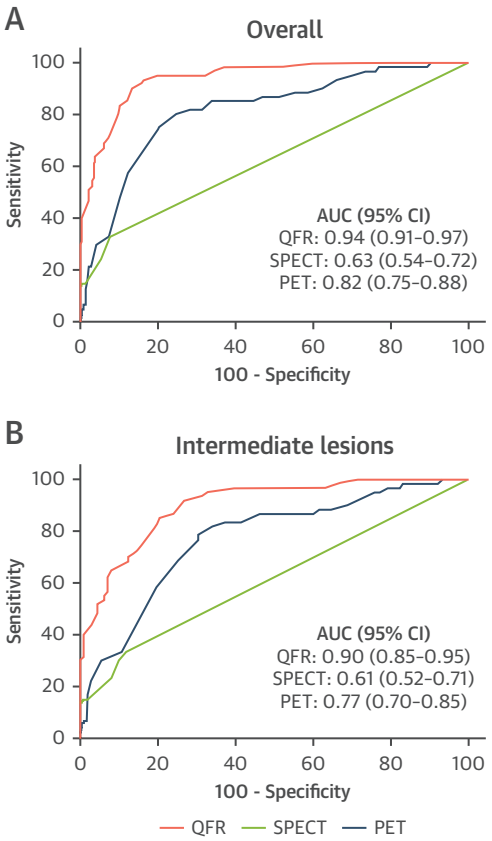

Receiver-operating characteristic curves with corresponding area under the curves (AUC) demonstrating the performance of QFR, single-photon emission computed tomography (SPECT), and positron emission tomography (PET) to assess per-vessel FFR-defined significant coronary artery disease, **(A)** overall and **(B)** among vessels with an intermediate lesion.
CI = confidence interval; other abbreviation as in Figure 1.

FIGURE 3 Correlation and Agreement Between QFR and FFR, Overall and Among Vessels With an Intermediate Lesion

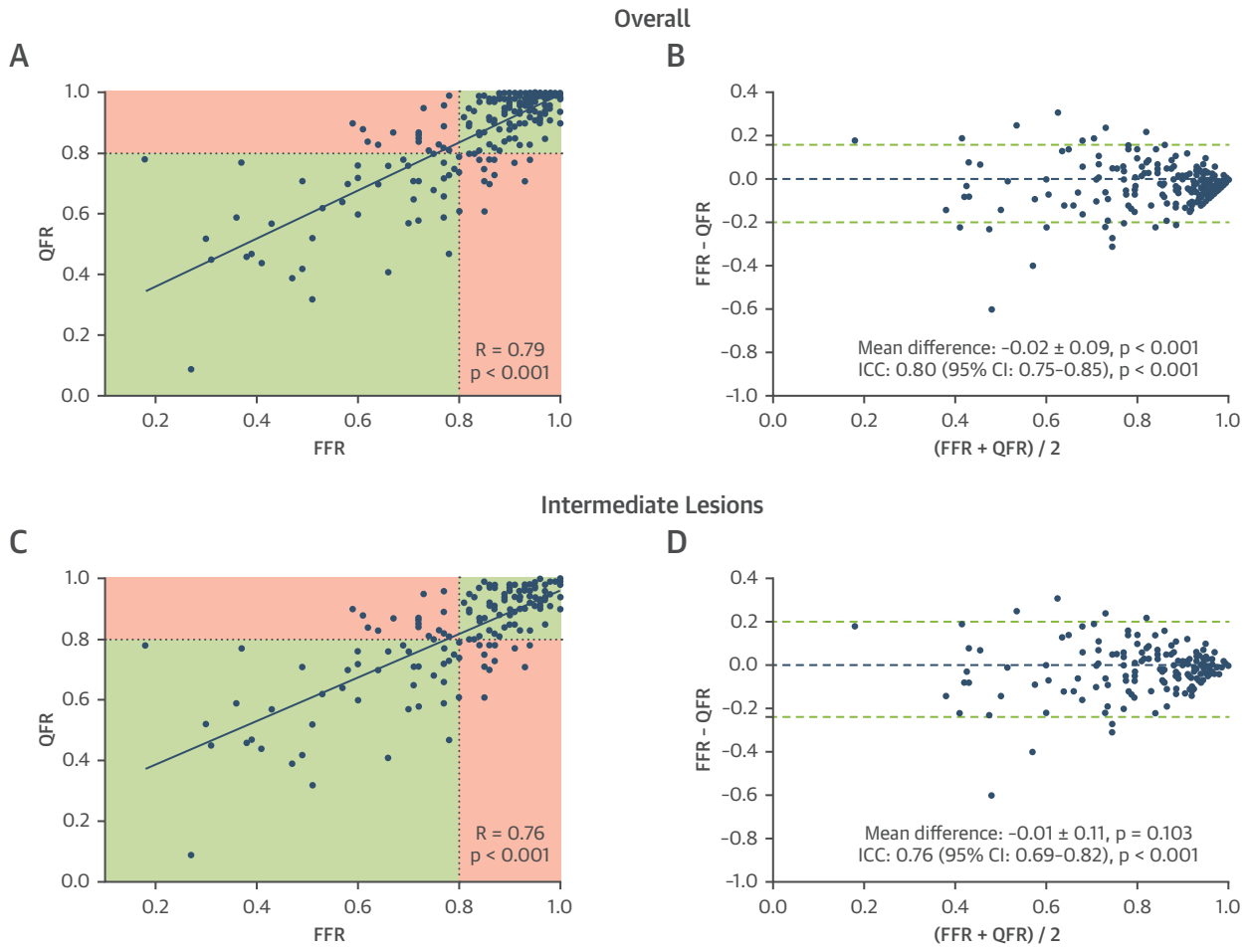

Scatterplots with corresponding Spearman R correlations coefficients and Bland-Altman plots with intraclass coefficients (ICCs) demonstrating the correlation and level of agreement between QFR and FFR, **(A to B)** overall and **(C to D)** among vessels with an intermediate lesion. Abbreviations as in Figures 1 and 2.

high clinical likelihood of CAD (2). The results of the present study, although exploratory in nature, indicated that a direct invasive approach using QFR might lead to a higher per-vessel diagnostic certainty compared with noninvasive MPI when referenced by FFR. Furthermore, when intermediate lesions were observed on ICA among patients without previous ischemia detection, subsequent MPI does not seem to have a beneficial effect in terms of improved diagnostic accuracy compared with direct interrogation by QFR. On the downside, QFR requires ICA, which is an invasive procedure with inherent albeit low risk of serious complications (e.g., myocardial infarction, stroke, and even death) (16). The risk of experiencing these detrimental events does not apply to noninvasive imaging techniques, as such patient counseling before choosing a diagnostic pathway, is vital. Another clinical scenario in which both an invasive approach and a noninvasive diagnostic strategy are feasible is the functional assessment of nonculprit lesions (NCL) in patients with ST-segment elevation myocardial infarction (17). QFR computation of NCLs based on ICA of the primary intervention demonstrates a high diagnostic accuracy when referenced by staged-FFR (18,19), comparable to the diagnostic accuracy observed among patients with stable CAD (18). In addition, immediate QFR also has good agreement with immediate FFR (accuracy: 94%) (20). Limited data are available on the ability of noninvasive MPI to assess the functional significance of NCLs, which has not been attempted with SPECT or PET, to the best of our knowledge. However, assessment of NCLs with noninvasive MPI by cardiac magnetic resonance has been undertaken and demonstrated a

FIGURE 4 **Correlation and Agreement Between QFR and FFR, Stratified According to Vascular Territory**

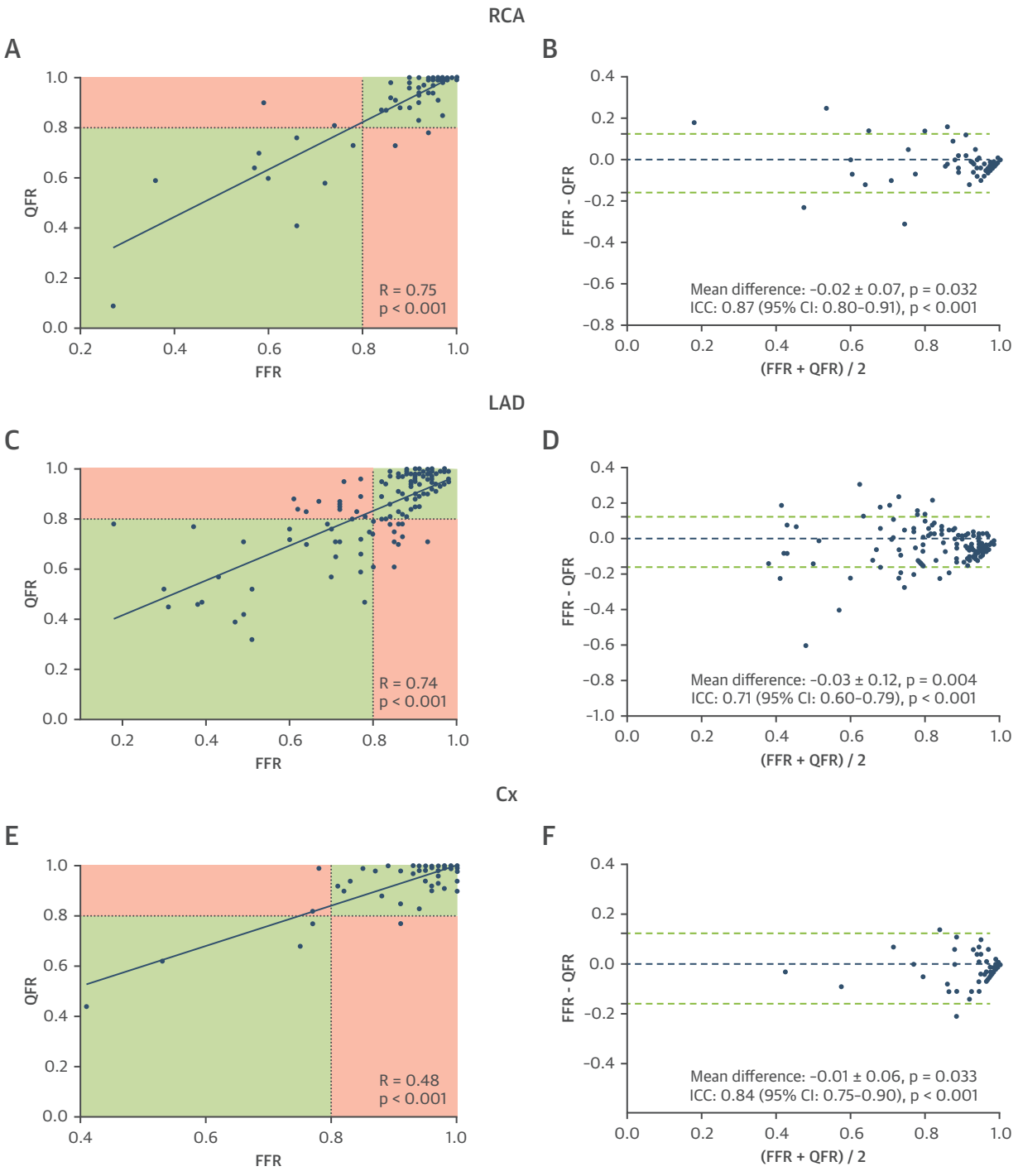

Scatterplots with corresponding Spearman R correlations coefficients and Bland-Altman plots with ICCs demonstrating the correlation and level of agreement between QFR and FFR per vascular territory: **(A, B)** RCA, **(C, D)** left anterior descending artery (LAD), and **(E, F)** left circumflex artery (Cx). Abbreviations as in Figures 1 to 3.

CENTRAL ILLUSTRATION **Diagnostic Comparison Between QFR and Perfusion Imaging**

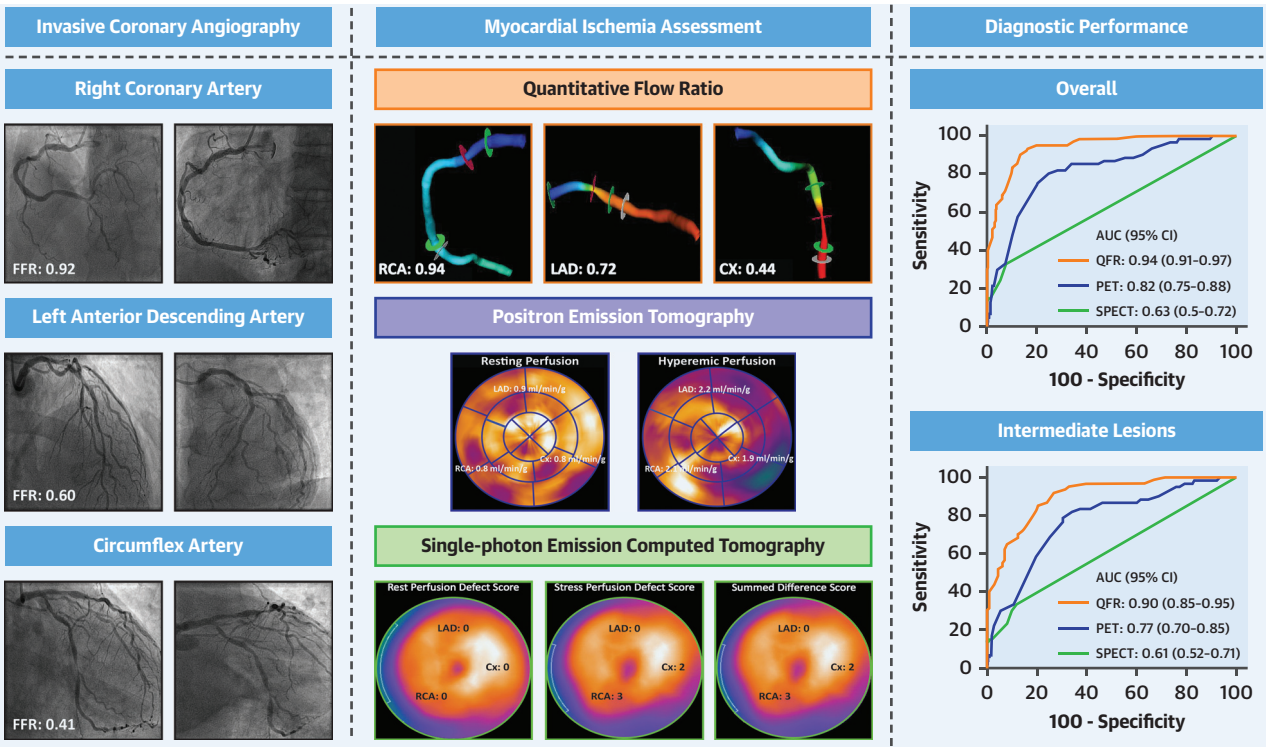

van Diemen, P.A. et al. J Am Coll Cardiol Img. 2020;13(9):1976–85.

The ability of quantitative flow ratio (QFR) (≤0.80) to assess fractional flow reserved (FFR)–defined significant coronary artery disease (FFR ≤0.80) was compared with single-photon emission computed tomography (SPECT) (summed difference score ≥2) and [^{15}O]H_2O positron emission tomography (PET) (hyperemic perfusion ≤2.3 ml/min/g in at least 2 adjacent segments). Patients (n = 208) underwent SPECT and PET before invasive coronary angiography in conjunction with FFR. QFR computation was retrospectively attempted and successful in 286 (52%) of the vessels in which FFR was obtained (552 vessels); of these vessels, 60% had a lesion of intermediate severity. The areas under the curve (AUC) demonstrate QFR exhibited a superior diagnostic performance in comparison to SPECT and PET for assessing FFR-defined ischemia. CI = confidence interval; CX = left circumflex artery; LAD = left anterior descending artery; RCA = right coronary artery.

vessel accuracy of 75% when referenced to staged FFR (21). Prospective comparative studies are necessary to determine whether QFR or MPI has superior diagnostic value and improves patient outcome when assessing NCLs in the setting of ST-segment elevation myocardial infarction.

STUDY LIMITATIONS. First, ICA in the PACIFIC trial was obtained without adherence to a dedicated QFR acquisition protocol; therefore, QFR could not be analyzed in 48% of the vessels, which hampered a per-patient and intention-to-diagnose analysis. Furthermore, in general, QFR computation is not validated in patients with atrial fibrillation, bifurcation lesions with a medina 1,1,1 classification, ostial left main or ostial right coronary artery stenosis, and grafted arteries. Second, although the definition of ischemia on SPECT is based on international guidelines and the applied PET threshold is considered the optimal cutoff to discern FFR-defined significant CAD, results of the present study might differ when alternate thresholds are used (11,14,22). Third, the present study focused on the diagnostic performance in terms of sensitivity, specificity, and accuracy, which are dependent on the precision of the modalities to assess FFR but also dependent on FFR distribution within a population. Therefore, accuracy will be higher in a population with FFR values far away from the threshold and will be lower when FFR is clustered around the threshold (Supplemental Table 2). As such, the present results should be interpreted in light of the studied population, that is, patients with an intermediate probability of CAD. Last, although the impact of individualized segmentation on the diagnostic performance of PET was negligible, discordance between the standardized American Heart Association 17-segment model used for MPI and true anatomy could not be ruled out (23).

CONCLUSIONS

In this head-to-head comparative study, QFR computation was successful in 52% of the vessels. Among these vessels, QFR demonstrated a higher diagnostic value for determining FFR-defined, lesion-specific ischemia compared with SPECT and PET. Even among vessels with an intermediate stenosis, QFR continued to accurately discern the hemodynamic significance of CAD. Prospective studies using a dedicated QFR acquisition protocol are warranted to assess the per-patient and intention-to-diagnose performance of QFR compared with noninvasive MPI.

ADDRESS FOR CORRESPONDENCE: Dr. Paul Knaapen, Department of Cardiology, Amsterdam UMC, Vrije Universiteit Amsterdam, De Boelelaan 1117, 1081 HV Amsterdam, the Netherlands. E-mail: p.knaapen@amsterdamumc.nl.

PERSPECTIVES

COMPETENCY IN MEDICAL KNOWLEDGE: For patients with suspected CAD who had both an invasive and noninvasive functional diagnostic strategies feasible, a direct invasive approach using QFR might lead to a higher per-vessel diagnostic certainty compared with noninvasive MPI by SPECT or PET.

TRANSLATIONAL OUTLOOK: Prospective studies comparing QFR with noninvasive functional tests are needed to assess the per-patient diagnostic performance and potential superiority of QFR over noninvasive ischemia detection.

REFERENCES

1. Tonino PAL, De Bruyne B, Pijls NHJ, et al. Fractional flow reserve versus angiography for guiding percutaneous coronary intervention. N Engl J Med 2009;360:213–24.

2. Knuuti J, Wijns W, Saraste A, et al. 2019 ESC guidelines for the diagnosis and management of chronic coronary syndromes. Eur Heart J 2019;00:1–71.

3. Tu SX, Barbato E, Kooszegi Z, et al. Fractional flow reserve calculation from 3-dimensional quantitative coronary angiography and TIMI frame count. J Am Coll Cardiol Intv 2014;7:768–77.

4. Westra J, Andersen BK, Campo G, et al. Diagnostic performance of in-procedure angiography-derived quantitative flow reserve compared to pressure-derived fractional flow reserve: the FAVOR II Europe-Japan Study. J Am Heart Assoc 2018;7:e009603.

5. Xu B, Tu SX, Qiao SB, et al. Diagnostic accuracy of angiography-based quantitative flow ratio measurements for online assessment of coronary stenosis. J Am Coll Cardiol 2017;70:3077–87.

6. Driessen RS, Raijmakers PG, Stuijfzand WJ, Knaapen P. Myocardial perfusion imaging with PET. Int J Cardiovasc Imaging 2017;33:1021–31.

7. Danad I, Raijmakers PG, Driessen RS, et al. Comparison of coronary CT angiography, SPECT, PET, and hybrid imaging for diagnosis of ischemic heart disease determined by fractional flow reserve. JAMA Cardiol 2017;2:1100–7.

8. Cerqueira MD, Weissman NJ, Dilsizian V, et al. Standardized myocardial segmentation and nomenclature for tomographic imaging of the heart - a statement for healthcare professionals from the Cardiac Imaging Committee of the Council on Clinical Cardiology of the American Heart Association. Circulation 2002;105:539–42.

9. Westra J, Tu S, Campo G, et al. Diagnostic performance of quantitative flow ratio in prospectively enrolled patients: an individual patient-data meta-analysis. Catheter Cardiovasc Interv 2019;94:693–701.

10. Westra J, Tu SX, Winther S, et al. Evaluation of coronary artery stenosis by quantitative flow ratio during invasive coronary angiography the WIFI II study (Wire-Free Functional Imaging II). Circ Cardiovasc Imag 2018;11:e007107.

11. Danad I, Uusitalo V, Kero T, et al. Quantitative assessment of myocardial perfusion in the detection of significant coronary artery disease: cutoff values and diagnostic accuracy of quantitative [(15)O]H2O PET imaging. J Am Coll Cardiol 2014;64:1464–75.

12. de Waard GA, Danad I, Petraco R, et al. Fractional flow reserve, instantaneous wave-free ratio, and resting Pd/Pa compared with [15O]H2O positron emission tomography myocardial perfusion imaging: a PACIFIC trial sub-study. Eur Heart J 2018;39:4072–81.

13. Xaplanteris P, Fournier S, Pijls NHJ, et al. Five-year outcomes with PCI guided by fractional flow reserve. N Engl J Med 2018;379:250–9.

14. Sand NPR, Veien KT, Nielsen SS, et al. Prospective comparison of FFR derived from coronary CT angiography with SPECT perfusion imaging in stable coronary artery disease: the ReASSESS study. J Am Coll Cardiol Img 2018;11:1640–50.

15. Nissen L, Winther S, Westra J, et al. Diagnosing coronary artery disease after a positive coronary computed tomography angiography: the DanNICAD open label, parallel, head to head, randomized controlled diagnostic accuracy trial of cardiovascular magnetic resonance and myocardial perfusion scintigraphy. Eur Heart J Cardiol Img 2018;19:369–77.

16. Tavakol M, Ashraf S, Brener SJ. Risks and complications of coronary angiography: a comprehensive review. Glob J Health Sci 2012;4:65–93.

17. Vogel B, Mehta SR, Mehran R. Reperfusion strategies in acute myocardial infarction and multivessel disease. Nat Rev Cardiol 2017;14:665–78.

18. Lauri F, Macaya F, Mejia-Renteria H, et al. Angiography-derived functional assessment of non-culprit coronary stenoses during primary percutaneous coronary intervention for ST-elevation myocardial infarction. EuroIntervention 2020;15:e1594–601.

19. Sejr-Hansen M, Westra J, Thim T, et al. Quantitative flow ratio for immediate assessment of nonculprit lesions in patients with ST-segment elevation myocardial infarction-an iSTEMI substudy. Catheter Cardiovasc Interv 2019;94:686–92.

20. Spitaleri G, Tebaldi M, Biscaglia S, et al. Quantitative flow ratio identifies nonculprit coronary lesions requiring revascularization in patients with ST-segment-elevation myocardial infarction and multivessel disease. Circ Cardiovasc Intervention 2018;11:e006023.

21. Everaars H, van der Hoeven NW, Janssens GN, et al. Cardiac magnetic resonance for evaluating nonculprit lesions after myocardial infarction: comparison with fractional flow reserve. J Am Coll Cardiol Img 2019;13:715–28.

22. Tilkemeier PL, Bourque J, Doukky R, Sanghani R, Weinberg RL. ASNC imaging guidelines for nuclear cardiology procedures. J Nucl Cardiol 2017;24:2064–128.

23. Bom MJ, Schumacher SP, Driessen RS, et al. Impact of individualized segmentation on diagnostic performance of quantitative positron emission tomography for haemodynamically significant coronary artery disease. Eur Heart J Cardiovasc Imaging 2019;20:525–32.

KEY WORDS fractional flow reserve, positron emission tomography, quantitative flow ratio, single-photon emission computed tomography

APPENDIX For supplemental tables, please see the online version of this paper.